

## MEASUREMENT OF DEEP INELASTIC COMPTON SCATTERING OF HIGH ENERGY PHOTONS

NA 14 Collaboration

P. ASTBURY<sup>c</sup>, E. AUGÉ<sup>d</sup>, R. BARATE<sup>b</sup>, P. BAREYRE<sup>g</sup>, P. BENKHEIRI<sup>e</sup>, D. BLOCH<sup>1</sup>,  
P. BONAMY<sup>g</sup>, P. BORGEAUD<sup>g</sup>, B. BOUQUET<sup>d</sup>, J.M. BROM<sup>i</sup>, J.M. BRUNET<sup>f</sup>, H. BURMEISTER<sup>b</sup>,  
M. BURTCHELL<sup>c</sup>, S. COSTA RAMOS<sup>e</sup>, F. COUCHOT<sup>d</sup>, B. D'ALMAGNE<sup>d</sup>, M. DAVID<sup>g</sup>,  
A. DE BELLEFON<sup>f</sup>, A. DE LESQUENS<sup>g</sup>, P. DELLO RUSSO<sup>i,1</sup>, A. DUANE<sup>c</sup>, J.P. ENGEL<sup>i</sup>,  
J. ENGELEN<sup>b</sup>, A. FERRER<sup>d</sup>, T.A. FILIPPAS<sup>a</sup>, E. FOKITIS<sup>a</sup>, P. FRENKIEL<sup>f</sup>, E.N. GAZIS<sup>a</sup>,  
J. GIOMATARIS<sup>a</sup>, M. GORSKI<sup>k</sup>, P. GREGORY<sup>c</sup>, W. GURYN<sup>d,2</sup>, J.L. GUYONNET<sup>i</sup>, T. HOFMOKL<sup>j</sup>,  
A. JACHOLKOWSKA<sup>j</sup>, E.C. KATSOUFIS<sup>a</sup>, J. KENT<sup>f</sup>, P. KYBERD<sup>c,3</sup>, B. LEFIEVRE<sup>f</sup>, R. LEGENDRE<sup>g</sup>,  
Y. LEMOIGNE<sup>g</sup>, K. MAESHIMA<sup>b</sup>, T. MARSHALL<sup>g,4</sup>, J.G. McEWEN<sup>h</sup>, J. MORRIS<sup>c,5</sup>,  
P. MOUZOURAKIS<sup>d,6</sup>, R. NAMJOSHI<sup>c,7</sup>, B. NANDI<sup>c,8</sup>, Ph. NOON<sup>c</sup>, S. ORENSTEIN<sup>f,9</sup>,  
T. PAPADOPOULOU<sup>a</sup>, J.B.M. PATTISON<sup>b</sup>, P. PETROFF<sup>d</sup>, D. POUTOT<sup>f</sup>, P.G. RANCOITA<sup>g,10</sup>,  
F. RICHARD<sup>d</sup>, P. ROUDEAU<sup>d</sup>, A. ROUGE<sup>e</sup>, M. SCHAEFFER<sup>i</sup>, Ch. SEEZ<sup>c</sup>, H. SHOOSHTARI<sup>h</sup>,  
I. SIOTIS<sup>c</sup>, J. SIX<sup>d</sup>, Ch. TRAKKAS<sup>a</sup>, D. TREILLE<sup>b</sup>, G. TRISTRAM<sup>f</sup>, L.V. VAN ROSSUM<sup>g</sup>,  
G. VILLET<sup>g</sup>, T.S. VIRDEE<sup>c</sup>, A. VOLTE<sup>f</sup>, D.M. WEBSDALE<sup>c</sup>, J. WEST<sup>c,11</sup>, M. WINTER<sup>b,12</sup>,  
W. WOJCIK<sup>b,13</sup>, G. WORMSER<sup>d</sup>, J.P. WUTHRICK<sup>e</sup> and Y. ZOLNIEROWSKI<sup>g</sup>

<sup>a</sup> National Technical University, Athens, Greece

<sup>b</sup> CERN, Geneva, Switzerland

<sup>c</sup> Imperial College, London UK

<sup>d</sup> Linear Accelerator Laboratory (LAL), Orsay, France

<sup>e</sup> Ecole Polytechnique LPNHE, Palaiseau, France

<sup>f</sup> Collège de France, Paris, France

<sup>g</sup> DPHPE, Saclay, France

<sup>h</sup> University of Southampton, Southampton, UK

<sup>i</sup> CRN et Université Louis Pasteur, Strasbourg, France

<sup>j</sup> Institute of Experimental Physics, University of Warsaw, Warsaw, Poland

<sup>k</sup> Institute for Nuclear Studies, Warsaw, Poland

Received 5 January 1985

We present the first results on inclusive photo-production of prompt photons at high transverse momenta. The data were taken in an open spectrometer at CERN using a high intensity photon beam with energy between 50 and 150 GeV. After subtracting the yield of photons from indirect sources, a clear excess is observed for transverse momenta above 2.5 GeV/c. Deep inelastic Compton scattering with appropriate QCD corrections account for this excess. The data disfavour the gauge integer charge quark models so far proposed.

<sup>1</sup> Elettronica Progetti, Bari, Italy.

<sup>2</sup> Present address: Brookhaven National Laboratory, Upton, NY, USA.

<sup>3</sup> Present address: Queen Mary College, London, UK.

<sup>4</sup> On leave from Indiana University, Bloomington, IN, USA.

<sup>5</sup> Present address: Logica Ltd, UK.

<sup>6</sup> Present address: European Parliament, Brussels, Belgium.

<sup>7</sup> Present address: Rutgers University, New Brunswick, NJ, USA.

<sup>8</sup> Present address: Institute of Electrical Engineers, Harlow, UK.

<sup>9</sup> On leave from City College, New York, NY, USA.

<sup>10</sup> On leave from INFN-Milano, Milan, Italy.

<sup>11</sup> Present address: IBM Laboratories, Eastleigh, UK.

<sup>12</sup> Present address: CRN, Strasbourg, France.

<sup>13</sup> Present address: CCPN, Paris, France.

**Introduction.** Deep inelastic scattering using incident photons has long been considered a fundamental hard scattering process [1]. A manifestation of such a process is QED Compton scattering (QEDC), the elastic scattering of photons on quarks. The cross section for this process can be calculated with the nucleon structure function as the only input and is proportional to the fourth power of the quark electric charge. This two real photon process thus provides a way of measuring the electric charge of quarks.

In addition to the QEDC Born term, QCD processes can also lead to a high- $p_T$  photon in the final state. Recent calculations [2] show that terms beyond the leading logarithm approximation are small. The direct coupling of photons to hadron constituents for high- $p_T$  reactions like QEDC means that fewer structure and fragmentation functions are required as compared with hadro-produced reactions. Effects due to primordial transverse momenta of constituents are less significant. There are also fewer subprocesses which lead to any given initial and final state enabling clearer identification of processes involved at the parton level. Furthermore the higher order calculations contain fewer uncertainties.

Previously this reaction has been explored at low incident energy and low transverse momenta [3]. This letter presents the first data on inclusive photon production in a kinetical domain which allows a meaningful comparison with theory. This was possible with the advent of a high energy and high intensity photon beam in the CERN SPS North area.

**Experimental details.** The experiment was performed in the E12  $e-\gamma$  beam at the CERN SPS using the NA14 spectrometer. The layout of the spectrometer is shown in fig. 1 and a detailed description of the spectrometer and the beam line can be found in refs. [4].

A bremsstrahlung photon beam is derived from a broadband electron beam of mean energy 140 GeV and intensity of  $10^8$   $e^-$ /SPS pulse crossing a 10%  $X_0$  radiator. Photons above  $\sim 50$  GeV are tagged yielding a beam of mean energy of 80 GeV but extending up to  $\sim 150$  GeV. The experimental target is isoscalar ( $Li^6$ ) having a thickness corresponding to 10%  $X_0$ .

The spectrometer has a large angular acceptance to charged particles and photons. MWPC's in between and downstream of the two analysing magnets allow the measurement of particle momenta up to  $\sim 100$  GeV/c. The electron-gamma detector consists of three calorimeters which cover a polar angle up to 275 mrad in the laboratory. The forward and backward regions in the centre of mass are covered by calorimeters labelled FC and BC respectively and consist of lead-glass blocks. The intermediate region is covered by a lead scintillator sandwich and is labelled IC. MWPC's and calorimeters are desensitized in the horizontal plane to avoid electromagnetic background from pairs. The salient parameters of the three calorimeters are listed in table 1.

A fast minimum bias pretrigger provides a strobe for the experiment with a time jitter of less than 1 ns. It triggers mostly (90%) on electromagnetic background

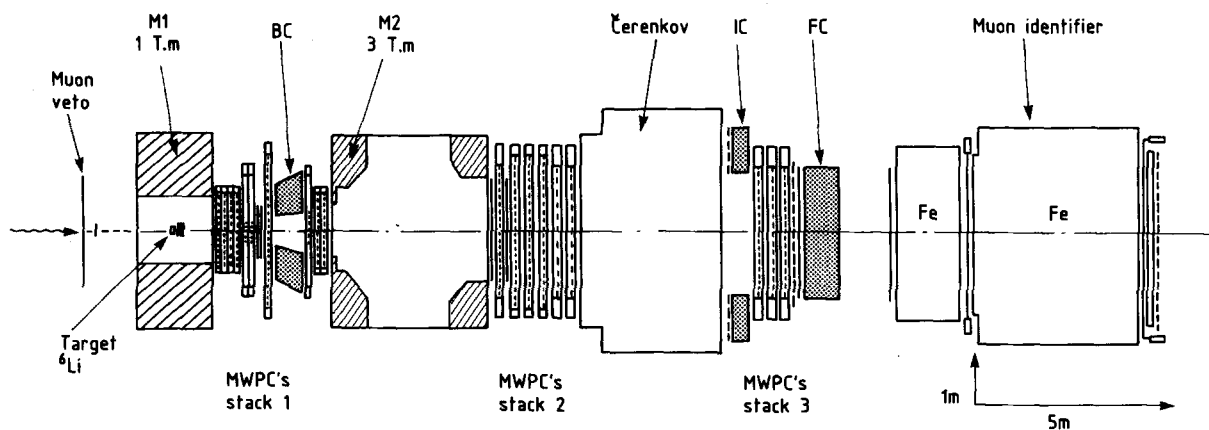


Fig. 1. Side view of the NA 14 spectrometer

Table 1  
Relevant parameters for the Na14 calorimeters.

	Calorimeter		
	FC forward	IC intermediate	BC backward
distance from target [cm]	1550	1350	240
coverage $\theta_{\text{LAB}}$ [mrad]	6.5–80	80–150	0 <sub>H</sub> , 80 <sub>V</sub> –275
$\theta$ ( $\gamma N \rightarrow \gamma X$ ) (100 GeV) [deg]	5–60	60–95	0 <sub>H</sub> , 60 <sub>V</sub> –125
converter before	active	active	passive
positron detector	$3X_0$ Pb glass	$4.5X_0$ Pb scintillator	$4.5 X_0$ lead
position detector		$y \cdot z$ crossed scintillator fingers	
finger width [cm]	1.5	1.5	0.8
material for			
total absorption	Pb glass	Pb scintillator	Pb glass
cell size [cm <sup>2</sup> ]	$14 \times 14$	25 cm in projection	$9.3 \times 9.3$
charged veto		scintillator matched to cell size	MWPC's
expected energy			
range for $\gamma, \pi^0$ [GeV]	$\leq 100$	$\leq 45$	$\leq 35$
minimal $2\gamma$ separation to be resolved [cm]	4.2	9	1.9
two-shower separation for 50% probability of resolution per projection [cm]	4	5	1.9
width of $\pi^0(\sigma)$ [MeV]	8.5	12.7	12.7
timing resolution, $\sigma$ [ns]	1.7	2.0	1.7
$\eta$ mass [MeV] (error is statistical)	$546 \pm 0.5$		$549 \pm 3$
$E/p$ for electrons (raw)	0.980	0.975	
minimal reconstructed energy [GeV]	1.5	1.5	0.85

but has full acceptance for hadronic events except for elastic production of  $\rho$ ,  $\omega$  and  $\phi$ . The data presented here come from a trigger which required, in addition to the pretrigger, a local deposit of energy in a calorimeter corresponding to a transverse momentum greater than 900 MeV/c. The high granularity of the calorimeters allowed us to trigger on single electromagnetic showers instead of a global transverse energy deposit.

The integrated luminosity is obtained by three independent methods which mutually agree within the errors. They use:

(i) A special trigger requiring at least two charged particles in opposite hemispheres that is sensitive to a known fraction of the total hadronic cross section.

(ii) The measurement of dimuon production in our apparatus.

(iii) The integrated flux of incident electrons.

We estimate that the uncertainty in the absolute normalisation is  $\pm 20\%$ . The data presented here correspond to a sensitivity of  $\sim 1.7$  events/pb above  $E_\gamma = 50$  GeV.

The energy calibration of the calorimeters was carried out by using reconstructed  $\pi^0$ 's. The width of  $\pi^0$  and  $\eta$  mass peaks is in agreement with the expected mass resolution. The absolute calibration is fixed by the  $\pi^0$  mass and is checked by the observed  $\eta$  mass and/or the measured ratio of energy over momentum for electron tracks. The systematic uncertainty in the energy calibration is estimated to be less than 3%. The error due to non-linearity in the calorimeter response in the photon energy range of interest is also estimated to be less than 3%.

*The prompt photon signal.* Photon candidates were

selected by requiring a lateral and longitudinal energy deposit in the calorimeter consistent with a single electromagnetic shower initiated by a neutral particle. In addition, the position detector and calorimeter cell information were required to be compatible with an impact of only one photon. The prompt photon candidate can be:

- i) A genuine prompt photon.
- ii) An indirect photon from a hadron decay or from the interaction of a neutral hadron (e.g. neutron,  $K_L^0$ ) giving an electromagnetic shower-like topology.
- iii) A shower initiated by a muon from the halo ( $\sim 10^6/m^2/s$ ) in random coincidence with the pretrigger and failing to give a signal in the charged vetoes in front of the candidate.

We reject the muon induced showers by a combination of the following cuts:

- (a) Applying a cut on the relative time of the pretrigger and the calorimeter hit.
- (b) Requiring no hit in the muon identifier hodoscopes directly behind the trigger cell (for FC and IC) or in an upstream beam halo veto counter (for BC).
- (c) Using additional spectrometer information to ensure that the photon candidate is part of a hadronic event thus rejecting 90% of the random triggers in-

duced by halo particles, since the pretrigger is only  $\sim 10\%$  hadronic.

The level of rejection has been verified by dumping the photon beam before the  $Li^6$  target and triggering as normal but with the pretrigger fulfilling only a beam requirement. It is found to be more than sufficient.

The largest source of background to prompt photons is due to indirect photons from  $\pi^0 \rightarrow \gamma\gamma$  and  $\eta \rightarrow \gamma\gamma$  decays. The dominant contribution comes from:

- (a) Photons from asymmetric decays where only the higher energy photon is observed in the calorimeter.
  - (b) Symmetric decays of high energy  $\pi^0$ 's such that the two shower separation is small and the presence of two distinct photons is not detected.
- Less important sources of background are:
- (c)  $\omega \rightarrow \pi^0\gamma$  and  $\eta' \rightarrow \gamma\gamma$  decays.
  - (d) Other neutral hadrons which leave electromagnetic shower-like topology.

The data from each calorimeter have been processed independently. For FC (BC) a  $p_L$  cut of 40 (10) GeV/c was imposed. The QEDC final state photon kinematics is shown in the CM plot of fig. 2. Since the iso-cross section contours have roughly the same

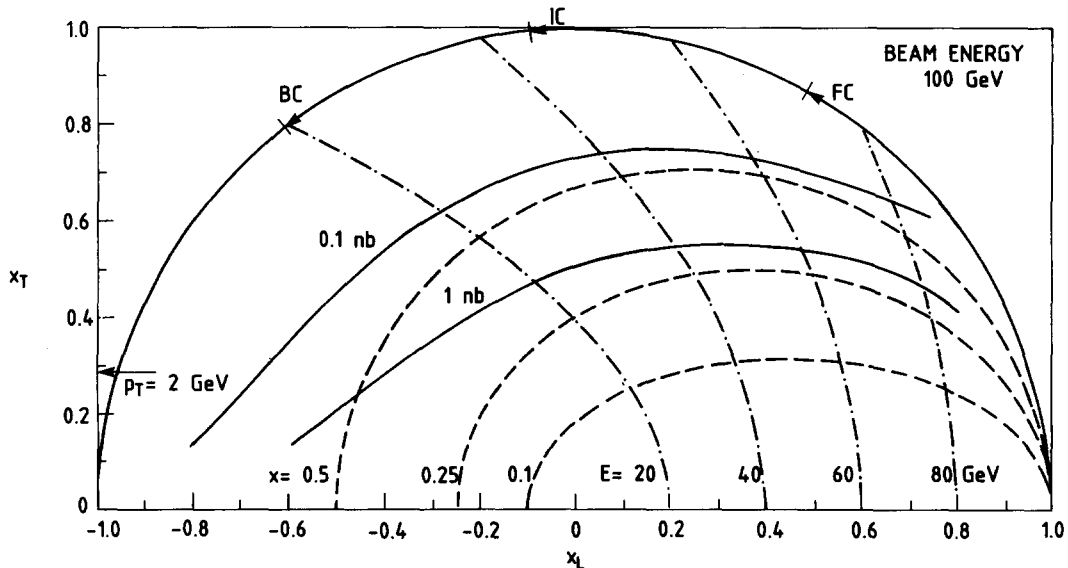


Fig. 2.  $x_T (=2p_T/\sqrt{s})$  versus  $x_L (=2p_L/\sqrt{s})$  plot with the geometric acceptance of the calorimeters in the centre of mass for a beam energy of 100 GeV. The solid lines show the contours of the differential cross section for QEDC Born term ( $\gamma q \rightarrow \gamma q$ ). Also shown are iso-energy (dashed and dotted line) and iso-x (dashed line) contours.

shape as iso- $x$  ones (where  $x$  is the fraction of the target nucleon momentum carried by the struck quark), it can be inferred from this figure that for FC both the energy range and mean energy of photon candidates varies weakly with  $p_T$ .

The background from indirect sources has been estimated by two independent methods:

(i) A classical method using detailed simulation of calorimeter response to showers relying as far as possible on data themselves.

(ii) A direct method which uses data taken in our spectrometer with an incident  $\pi^-$  beam.

(a) *The classical approach*: we use a Monte Carlo simulation program of the apparatus in order to evaluate the efficiency of reconstruction of a photon or a  $\pi^0$  and the probability that a  $\pi^0$  ( $\eta, \eta', \omega$ ) fakes a single photon. In addition we measure the inclusive  $\pi^0$  spectrum in the full kinematic domain and thus determine the inclusive  $\pi^0$  distribution at production. This distribution is then used as input to the Monte Carlo simulation in order to estimate the major source of background to prompt photons which comes from  $\pi^0 \rightarrow \gamma\gamma$  decays. The inclusive  $\pi^0$  measurement will be the subject of a subsequent publication.

Contamination from other indirect sources has been expressed as a fraction of that arising from neutral pions. In FC the  $\eta/\pi^0$  production ratio for  $p_T > 1.5$  GeV/c and  $p_L > 30$  GeV/c is found to be  $0.52 \pm 0.15$ , and we have used  $\eta/\pi^0 = 0.50$  corresponding to a weighted average of several hadro-production experiments [5]. We also assume that  $\eta'/\pi^0$  and  $\omega/\pi^0$  production ratios are 0.9 as found in an ISR experiment [6]. A change of  $\sim 20\%$  in  $\eta/\pi^0$  and a factor 2 in  $\eta'/\pi^0$  or (inelastic  $\omega$ )/ $\pi^0$  would not significantly modify the level of contamination.

Other neutral hadrons are efficiently eliminated when electromagnetic shower criteria are applied. This is confirmed by studying showers initiated by charged hadrons.

It is important to note that this method is independent of normalization and to a certain extent of acceptance.

We have applied it to the  $\pi^-$  induced data taken in the same experiment (see below), and find that the pio-produced inclusive  $\pi^0$  spectra are in good agreement with published data, both in  $p_T$  and  $p_L$  [7]. This represents a check of the reconstruction efficiency for  $\pi^0$ 's and, to a smaller extent, that for photons. We also

find that  $\gamma/\pi^0$  is less than 10% for the kinematical region considered here. This is consistent with measurements of several experiments on pio-production of prompt photons which find  $\gamma/\pi^0 \sim 3\%$  around  $p_T = 3$  GeV/c [8].

(b) *The direct method*: to determine empirically the non-prompt photon yield we use data taken with a  $\pi^-$  beam of 70, 90 and 120 GeV/c. Here we measure the number of reconstructed  $\pi^0$ 's and single photons, referred to as  $N(\pi^- \rightarrow \pi^0)$  and  $N(\pi^- \rightarrow \gamma)$ , and so determine the ratio  $F = N(\pi^- \rightarrow \gamma)/N(\pi^- \rightarrow \pi^0)$ .  $F$  can be a function of  $p_T$  and  $p_L$ . Carrying out the same measurements in a photon beam the prompt photon signal is

$$N(\gamma \rightarrow \gamma)_{\text{prompt}} = N(\gamma \rightarrow \gamma) - F \cdot N(\gamma \rightarrow \pi^0).$$

As an example, fig. 3 shows the results of the four measurements for IC.  $F$  is given by the ratio of curves in figs. 3b and 3a. In fig. 3d the curve corresponds to the background and is  $F$  times the curve of fig. 3c. In practice we have used a rigorous subtraction procedure requiring a bidimensional ( $p_T, p_L$ ) treatment. The simple picture described by fig. 3 turns out to be rigorously correct because for IC we find that the pio-produced and photo-produced  $\pi^0$  spectra have identical shapes in the ( $p_T, p_L$ ) plot.

In fig. 3d one can see the obvious presence of an extra component. It can also be seen for FC in fig. 4a. Fig. 4b shows the FC data versus  $p_L$ . The results for BC are shown in fig. 4d.

This subtraction method, as the previous one, is independent of normalization. Furthermore, it does not rely on any Monte Carlo evaluation of acceptance and contamination.

However, a few points had to be studied further:

(a) The  $\pi^-$  induced data used in the above comparison were taken in conditions where the muon halo flux was much smaller than in the photon induced data. This possible source of the difference between  $\gamma$  and  $\pi$  beam data was investigated by taking further  $\pi^-$  data with the same halo flux as in photon beam runs. We observe no difference in the single-photon yield up to the highest  $p_T$ 's between the two types of  $\pi^-$  beam data. We thus conclude that the halo induced background is well understood and eliminated. As an "a posteriori" proof of this, the impact distribution of our high- $p_T$  single-photon candidates is azimuthally uniform in both  $\gamma$  and  $\pi$  runs, whereas the muon flux

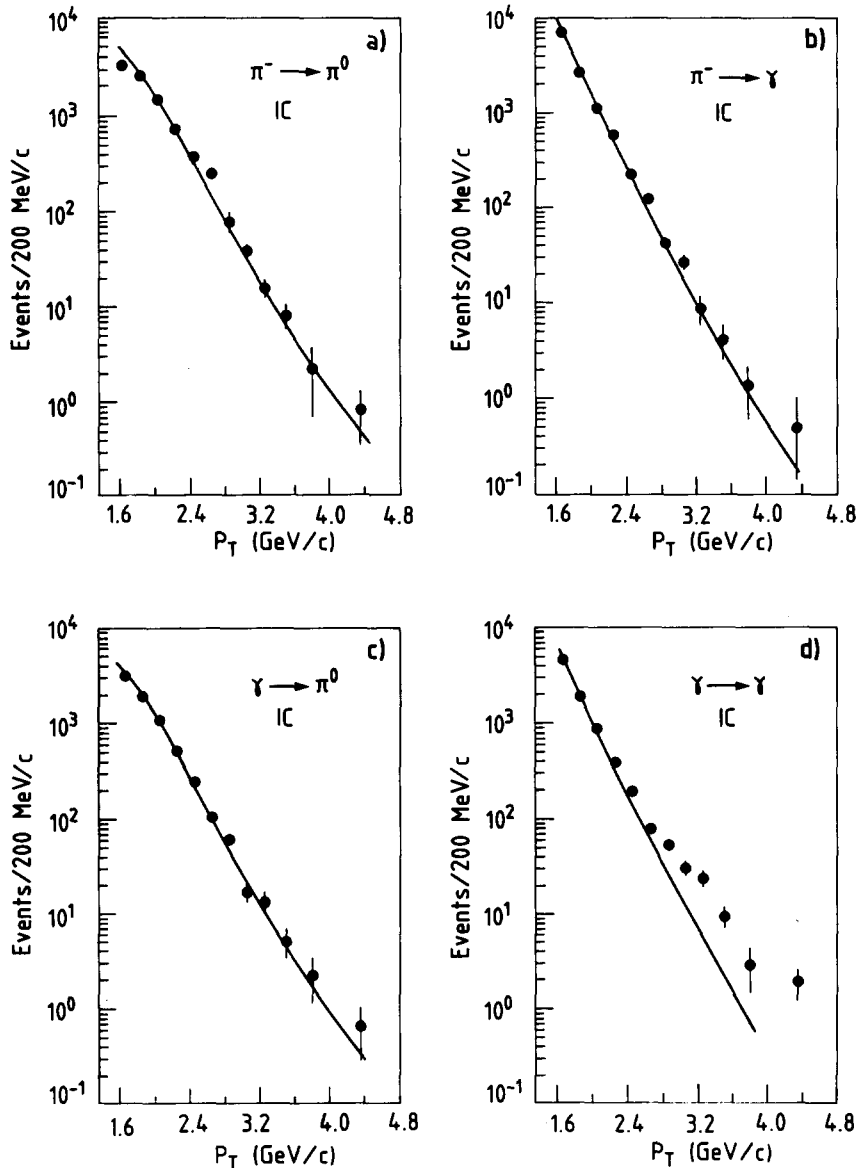


Fig. 3. Illustration of our empirical method to demonstrate the presence of a prompt photon signal. The shape of lines in (a) and (b) are obtained by Monte-Carlo using as input the cross section parametrization of ref. [7]. The overall normalisation in (a) has been adjusted to fit the data and agrees within 10% with that given by ref. [7]. For IC the shape of lines in (a) and (c) are identical. The line in (d) gives the indirect background and is obtained by computing  $[N(\pi^- \rightarrow \gamma)/N(\pi^- \rightarrow \pi^0)] \cdot N(\gamma \rightarrow \pi^0)$ .

density is highly non-uniform.

(b) A slight complication in the above procedure arises from the fact that the presence of genuine prompt photons in the pion-beam data will lead to a value of  $F$  which overestimates the indirect background

One can write  $F = F_{\text{direct}} + F_{\text{indirect}}$ . It is legitimate to apply  $F$  as a whole to the vector meson dominance (VMD) part of  $\pi^0$  photoproduction; this just implies that we subtract any source of prompt photons common to both pio- and photo-production. However,

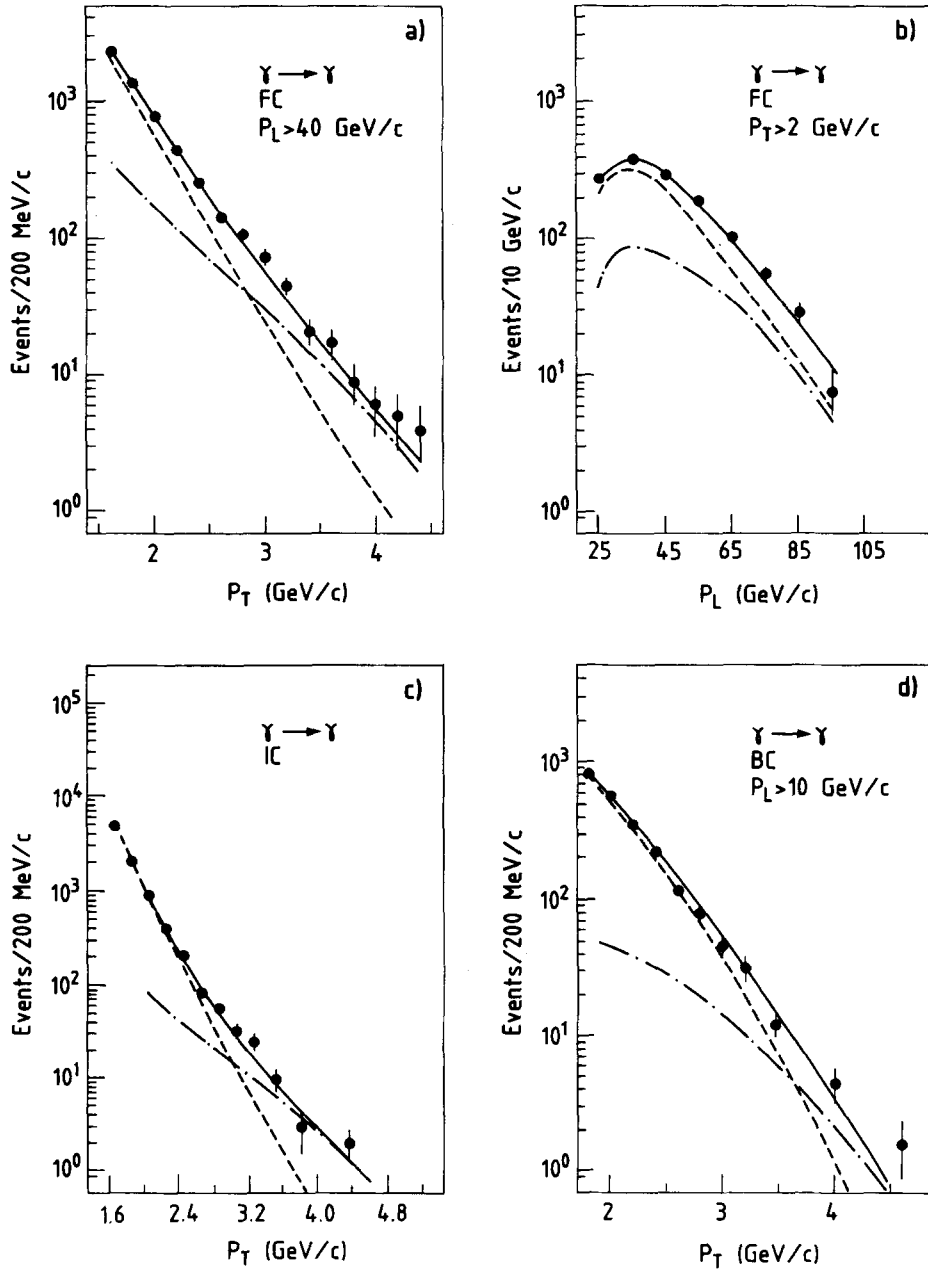


Fig. 4. The inclusive photon data compared with theoretical predictions. The dashed line corresponds to the background. The dashed-dotted line shows the magnitude of QED Compton Born and correction terms. The solid line represents the sum of background and theoretical prediction.

one should only apply  $F_{\text{indirect}}$  to the non VMD part of the  $\pi^0$  cross section. This problem arises in the forward region where a strong QCD component is observed in the photo-produced  $\pi^0$  spectrum. This correction leads to a 5% reduction in the level of the calculated background.

(c) In principle this direct method requires that  $\eta/\pi^0$ ,  $\eta'/\pi^0$ ,  $\omega$  (inelastic)/ $\pi^0$  etc. ratios are the same in pio- and photo-production. This has been verified for  $\eta$ 's: we have measured  $R_\eta = (\eta/\pi^0)_{\gamma \text{ beam}} / (\eta/\pi^0)_{\pi \text{ beam}}$  in a large part of the kinematic domain and find it to be  $1.2 \pm 0.3$  for  $p_T \sim 2.0$  GeV/c, consistent with unity. For the other ratios an unreasonably large change is required between pio- and photo-production to produce a significant change in the estimated background.

(d) In some kinematic regions, mainly at  $p_T$  and  $p_L$  in FC, the statistics from  $\pi^-$  induced runs were limited and we have used the Monte Carlo method to extrapolate to these regions.

The two methods of estimating the indirect  $\gamma$  background agree with each other to better than 10%.

In fig. 4 we show our results before background subtraction. The excess over background for FC and IC can be used to estimate the  $\gamma/\pi^0$  production ratio by using the Monte Carlo simulation of  $\pi^0$  and  $\gamma$  reconstruction efficiencies. The resulting ratio for FC and IC increases from  $\gamma/\pi^0 \sim 0.05$  at  $p_T \sim 2.0$  GeV/c ( $\sim 0.08$  if one adds the rate of VMD produced prompt  $\gamma$ ) to  $\sim 1.0$  at  $p_T \sim 4.0$  GeV/c. In fig. 5 we give the cross section for photo-production of prompt photons. It has been obtained from the combined data of FC and IC, integrated for rapidity  $y > -1$ , with the background subtracted.

The open geometry and the large acceptance of our spectrometer enables us to study event topologies. QED Compton events should have unaccompanied photons and a jet structure with a preponderance of positive leading particles opposite to single photons. The accompaniment, the jet structure and the charge asymmetry have been studied [9] and the results will be published in a future paper. The results indicate that QEDC-like events are present at a rate compatible with expectation from the inclusive analysis.

*Interpretation.* This section gives a detailed interpretation of our data in terms of QEDC scattering and additional contributions from perturbative QCD.

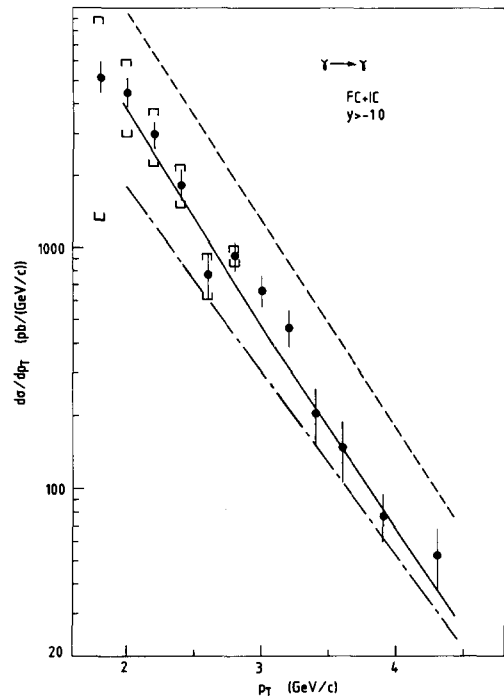


Fig. 5. The measured cross section for photo-production of prompt photons. The indirect background has been subtracted. The dashed-dotted and solid curves correspond to QEDC Born term and Born + correction terms respectively. The dashed curve is 2.65 times the solid curve. Also shown are systematic errors on the subtraction of background. The statistical errors dominate for  $p_T > 2.6$  GeV/c.

We have used the results of Aurenche et al. [2] and their computer code to generate photon momenta from QEDC scattering and higher order terms. They have evaluated the corrections to leading logarithm and next to leading order. They also include the contribution from the box diagram,  $\gamma\gamma \rightarrow \gamma\gamma$ . The magnitude of these corrections can be inferred from fig. 5.

We estimate that the combined uncertainty in absolute normalisation and photon reconstruction efficiency is less than 25%. The sum of Born and correction terms is shown as a dashed-dotted line in fig. 4. When added to our empirical determination of the background (dashed line) we obtain good agreement with the data.

In fig. 5 the dashed-dotted and solid lines correspond to QEDC Born term and Born term plus corrections, respectively. It can be seen that, for the

standard model with fractionally charged quarks (FCQ), the corrections play a substantial role in obtaining agreement with data.

In gauge integer charge quark models (ICQ) [10] <sup>+1</sup> colour symmetry is spontaneously broken and the electromagnetic charge of quarks acquires a colour octet component due to photon–gluon mixing. Coupling of virtual photons to this colour component is strongly suppressed (“colour damping” [12]) for values of the virtual photon mass bigger than the lagrangian mass ( $<200 \text{ MeV}/c^2$ ) that the gluons acquire in these models. Furthermore, below threshold for physical colour production, a single-photon process will always project the photon onto its singlet component and thus give the same result for both ICQ and FCQ. Hence *only processes involving at least two real photons* can efficiently distinguish between ICQ and FCQ. Some controversial points concerning quark charge measurement and ICQ models are discussed in refs. [13] and ref. [14], respectively. ICQ models [15] predict for the Born term a cross section which is 2.65 times larger <sup>+2</sup> than that for FCQ. The corrections for ICQ models equivalent to those calculated in ref. [2] for FCQ have not been computed. Lacking this information, we have multiplied the solid line in fig. 5 by 2.65 leading to the dashed line in the same figure and this prediction is ruled out by our data. The degree of rejection is determined essentially by the normalization error.

**Conclusion.** We have presented in this letter the first measurement of photoproduction of prompt photons in a kinematical domain allowing a meaningful comparison with theory. The QED Compton process with QCD corrections accounts for the observed level of prompt photon production. It is significant that the predicted magnitude of these corrections is in agreement with experiment. The data disfavour the gauge integer charge quark models proposed so far.

<sup>+1</sup> For a short and concise review of gauge integer charge models see ref. [11].

<sup>+2</sup> The ratio of the magnitude of Born terms, neglecting charged gluon contributions, is given by:  $\text{ICQ}/\text{FCQ} = \frac{\sum_f (3^{-1/2} \sum_c Q_{fc}^2)^2}{3 \sum_f Q_f^4}$ , where f stands for flavour and c for colour.

We sincerely thank the technical staffs of the Institutes collaborating in NA 14 for their invaluable contributions and are particularly indebted to L. Andersson, H. Atherton, C. Aubret, L. Bassi, F. Berny, G. Bouvard, W. Cameron, N. Doble, G. Dubail, G. Dubois-Dauphin, R. Ferlicot, C. Fritsch, J.P. Grillet, R. Harfield, D. Miller, J. Movchet, J. Pascual, J. Poinsignon, C. Sobczynski, J.P. Vanuxem, P. Vergezac. We gratefully acknowledge the work of the authors of our pattern recognition and track fitting program F. Carena, F. James, J.C. Lassalle and S. Pensotti. We thank R. Collet for assistance in tape handling. Finally we would like to thank M. Jouhet for preparing the manuscript.

### References

- [1] J.D. Bjorken and E.A. Paschos, Phys. Rev. 185 (1969) 1975.
- [2] P. Aurenche, R. Baier, A. Douiri, M. Fontannaz and D. Schiff, Z. Phys. C24 (1984) 309; D.W. Duke and J.F. Owens, Phys. Rev. D26 (1982) 1600; D28 (1983) 1227 (E).
- [3] D.O. Caldwell et al., Phys. Rev. Lett. 33 (1974) 868.
- [4] E. Augé, Thesis LAL Orsay 83/09; D. Bloch, Thesis CRN Strasbourg CRN/HE 82–03; F. Couchot, Thesis LAL Orsay 80/84; M. Winter, Thesis CRN Strasbourg, CRN/HE 81-03; C. Seez, Ph.D. Thesis Imperial College, London (1983), Rutherford Laboratory report HEP T 118.
- [5] J. Povlis et al., Phys. Rev. Lett. 51 (1983) 967; G. Donaldson et al., Phys. Rev. Lett. 40 (1978) 684; R.M. Baltrusaitis et al., Phys. Lett. 88B (1979) 372.
- [6] M. Diakonou et al., Phys. Lett. 89B (1980) 432.
- [7] G. Donaldson et al., Phys. Lett. 73B (1978) 375.
- [8] M. McLaughlin et al., Phys. Rev. Lett. 51 (1983) 971; J. Badier et al., CERN preprint CERN EP/84-101; K. Pretzl, talk XXII Intern. Conf. on High energy physics (Leipzig, 1984).
- [9] Ph. Noon, Ph. D. Thesis, Imperial College, London (1984); G. Wormser, Thesis LAL Orsay (December 1984).
- [10] J.C. Pati and A. Salam, Phys. Rev. D8 (1973) 1240; G.M. Vereshkov, S.A. Zharinov, S.V. Ivanov and S.V. Mikhailov, Sov. J. Nucl. Phys. 32 (1980) 1.
- [11] R.M. Godbole, J.C. Pati, S.D. Rindani, T. Jayaraman and G. Rajasekaran, Phys. Lett. 142B (1984) 91.
- [12] G. Rajasekaran and P. Roy, Pramana 6 (1975) 303; J.C. Pati and A. Salam, Phys. Rev. Lett. 36 (1976) 11.
- [13] H.J. Lipkin, Phys. Lett. 85B (1979) 236.
- [14] L.B. Okun, M.B. Voloshin and V.I. Zakharov, ITEP Moscow preprint ITEP-79 (1979).
- [15] A.V. Efremov, S.V. Ivanov and V.A. Nesterenko, JINR Dubna preprint E2-82-433 (1982).